REVISTA INTERDISCIPLINAR DE PESQUISA EM ENGENHARIA

CILAMCE 2016
XXXVII IBERIAN LATIN AMERICAN CONGRESS ON COMPUTATIONAL METHODS IN ENGINEERING
BRASÍLIA - DF - BRAZIL

COMPARISON BETWEEN THE CLASSICAL SUB REGIONS TECHNIQUE AND A NEW APPROACH WITH DOMAIN SUPERPOSITION TO SOLVE SECTORIAL INHOMOGENEOUS LAPLACE'S PROBLEMS

André Judá Correa de Andrade

Carlos Friedrich Loeffler

andrejudah@gmail.com

carlosloeffler@bol.com.br

Programa de Pós Graduação em Engenharia Mecânica, PPGEM/UFES

Av. Fernando Ferrari, 540 – Bairro Goiabeiras – 29075 – 910, Vitória, ES – Brasil

Abstract. The Boundary Element Method (BEM) has excellent performance in applications where the variable field is scalar and stationary. However, there is a wide range of issues in science and engineering that are difficult to solve by the BEM. Among these issues, there are the constitutive non-homogeneous problems, where the physical properties vary sectorally. In these kind of problems, the domain techniques, such as Finite Element Method (FEM), Finite Volume Method (FVM) or Finite Difference Method (FDM), present considerable advantages. However, even for these cases, there is a consistent BEM formulation, the classic sub-region technique. This work presents numerical comparisons between the classic sub-region technique and an alternative BEM technique that is not based on a partition of the domain. Results are compared with analytical results and other achieved by domain methods using finer meshes.

Keywords: *Boundary Element Method, Inhomogeneous Laplace's Problems, Sub-regions Technique*

1 INTRODUCTION

Let a stationary scalar field governing by Laplace's Equation, in which the physical properties are isotropic, but it is different in each sector of domain, such as shown schematically in Fig. 1:

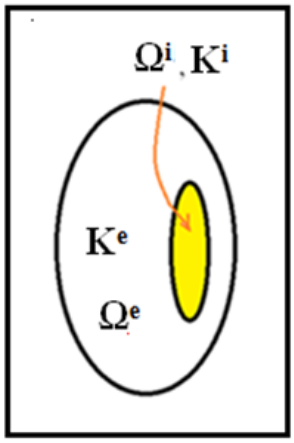

Figure 1: Sketch of a domain with sectorial inhomogeneous properties

In this case, the physical property Ke is assumed to be constant on each sub domain. There are many important engineering problems in which this model corresponds satisfactory with physical situations, such as soil mechanics problems, layered-materials analysis and thermal analysis of welding or similar processes of in manufacture in metals. Commonly, in this class of problems the domain numerical methods are easily preferred, since the physical property can be introduced directly in each sub domain. Oppositely, there is a relative difficulty to model these problems using the Boundary Element Method (BEM) in this standard form.

The use of classic sub-regions technique is still the most efficient approach (Brebbia et al., 1984) for this situation. The procedure is based on a very simple concept considering domain partition. Different sub-domains are analyzed separately and independent systems of equations are generated after the discretization procedure. Figure 2 illustrates a domain partitioned in two sub-regions:

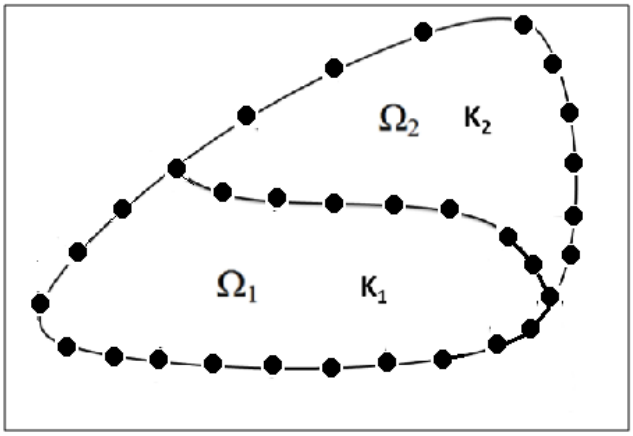

Figure 2: Division of complete domain in two sub-regions

However, due to the insertion of internal boundaries, an additional numerical approximation is introduced by the discretization. Beyond this, in certain complex situations, the sub-regions technique is unsatisfactory, because it becomes costly and inadequate for programming (Xiaoping and Wei-Liang, 2005).

There are other important engineering problems in which the partition of domain is required of some way, such as fracture analysis and plasticity problems. Despite the higher accuracy of the BEM in these cases, commonly resources such as cells are used. Unfortunately, there are no other efficient BEM approach regarding the solution of this important class of problems and meaningful changes were not observed concerning sub-regions technique along the time (Brebbia and Dominguez, 1992; Wrobel and Aliabadi, 2002).

This work presents an alternative to treat this category of problems that, due to its simplicity, can accredit the BEM to further elaborate applications without implementation difficulties. In a way the idea of this work is approximately presented in models that consider localized domain actions, which consist of another kind of problem for which the BEM requires additional auxiliary techniques to become efficient. Loeffler and Mansur (1987) used this approach to account for sectorial loads with Dual Reciprocity (Partridge et al., 1992).

Basically, the alternative procedure connect different sub-domains such as plates with columns in structures (Paiva and Venturini, 1993;) using internal points; however, the approach presented here since is more general, since theoretical considerations are presented to justify a model where the energy of each sub-domain is computed such as is done with a domain source in Poisson's problems.

Aiming to evaluate the performance of the proposed procedure, simple problems are solved and their numerical solutions are compared with results obtained by the classical sub-region technique.

2 SUB-REGIONS MODEL

The BEM inverse integral equation for the Laplace's problems is well known, being given by (Brebbia & Walker, 1980):

$$\mathbf{K}\left[\int_{\Gamma} \mathbf{q}(\mathbf{X})\mathbf{u}^{*}(\boldsymbol{\xi};\mathbf{X})\mathbf{d}\boldsymbol{\Gamma} - \int_{\Gamma} \mathbf{u}(\mathbf{X})\mathbf{q}^{*}(\boldsymbol{\xi};\mathbf{X})\mathbf{d}\boldsymbol{\Gamma} + \int_{\Omega} \mathbf{u}(\mathbf{X})\mathbf{u}^{*}_{,\mathbf{ii}}(\boldsymbol{\xi};\mathbf{X})\mathbf{d}\boldsymbol{\Omega}\right] = \mathbf{0} \qquad (1)$$

In Eq. (1), u(X) is the scalar potential and q(X) is its normal derivative; reciprocally, u*(ξ,X) is the fundamental solution for the Laplace equation and q*(ξ,X) is its normal derivative; K is the physical property that, for homogeneous problems, could be omitted. The coefficient c(ξ) depends on the position of point ξ in relation to the physical domain Ω(X)+ Γ(X), and if the point is located on the boundary Γ(X), it also depends on its smoothness (Kythe, 1995).

Considering finite domains, the essential and natural boundary conditions are prescribed on closed boundaries Γ(X), given respectively by the following equations:

$$u(\mathbf{X}) = \bar{u}(\mathbf{X}), \quad \text{on} \quad \Gamma_u(\mathbf{X}) \ ; \text{and} \ \ u_{,i}\, n_i(\mathbf{X}) = \bar{q}(\mathbf{X}), \quad \text{on} \quad \Gamma_q(\mathbf{X}) \qquad (2)$$

In Eq. 2 n_i is the unit outward normal vector on the boundary $\Gamma(X)$, that is composed by the union of boundary regions $\Gamma_u(X)$ and $\Gamma_q(X)$.

Application of mathematical procedures typical of BEM that includes a scanning on the boundary integrations, taken different source points located on the nodes, and also the discretization process, matrices H and G are generated as indicated below:

$$[H]\{u\} = [G]\{q\} \tag{3}$$

Considering two sub-regions for sake of simplicity, as illustrate in Fig. 3, equation (3) is generated separately for each sub-region, as written below:

$$[H^1 \quad H_I^1]\begin{Bmatrix} U^1 \\ U_I^1 \end{Bmatrix} = [G^1 \quad G_I^1]\begin{Bmatrix} Q^1 \\ Q_I^1 \end{Bmatrix} \tag{4}$$

$$[H^2 \quad H_I^2]\begin{Bmatrix} U^2 \\ U_I^2 \end{Bmatrix} = [G^2, \quad G_I^2]\begin{Bmatrix} Q^2 \\ Q_I^2 \end{Bmatrix} \tag{5}$$

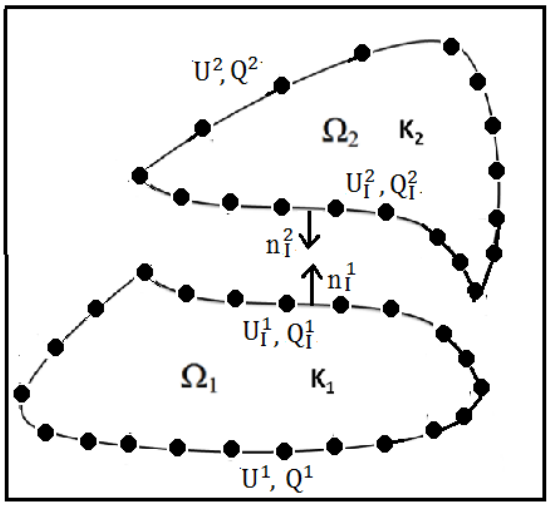

Figure 3: Domain partition in two sub-regions

In equation (4) and (5) H^1 and G^1, are submatrices related to nodes at external boundary 1; H^2 and G^2 are sub matrices related to nodes at external boundary 2; H^1_I and G^1_I are sub matrices generated by integrations related to nodes at interface 1; and H^2_I and G^2_I are submatrices generated by integrations related to nodes at interface 2.

The sub regions are linked by using compatibility and equilibrium conditions between in nodes of common interfaces (Ramachandran, 1994), that is:

$$U_I^1 = U_I^2 = U_I \tag{6}$$

$$Q_I^1 = -\frac{K_2}{K_1} Q_I^2 = Q_I \tag{7}$$

Appling conditions given by Eq. (6) and (7) at the interface nodes, a complete matrix system is achieved:

$$\begin{bmatrix} H^1 & H_I^1 & 0 \\ 0 & H_I^2 & H^2 \end{bmatrix} \begin{Bmatrix} U^1 \\ U_I \\ U^2 \end{Bmatrix} = \begin{bmatrix} G^1 & G_I^1 & 0 \\ 0 & -G_I^2 & G^2 \end{bmatrix} \begin{Bmatrix} Q^1 \\ Q_I \\ Q^2 \end{Bmatrix} \tag{8}$$

Remembering that both the potentials and their normal derivatives at the interface are considered as unknowns, the system given by Eq. can be rewritten as:

$$\begin{bmatrix} H^1 & H_I^1 & -G_I^1 & 0 \\ 0 & H_I^2 & G_I^2 & H^2 \end{bmatrix} \begin{Bmatrix} U^1 \\ U_I \\ Q_I \\ U^2 \end{Bmatrix} = \begin{bmatrix} G^1 & 0 \\ 0 & G^2 \end{bmatrix} \begin{Bmatrix} Q^1 \\ Q^2 \end{Bmatrix} \tag{9}$$

Notice that the final system matrix for sub-region technique is a banded matrix. This feature of matrix is increase for a greater number of sub-regions.

3 THE SUPERPOSITION TECHNIQUE

For instance, consider a domain composed by two regions with different physical properties, as shown in Fig. 4:

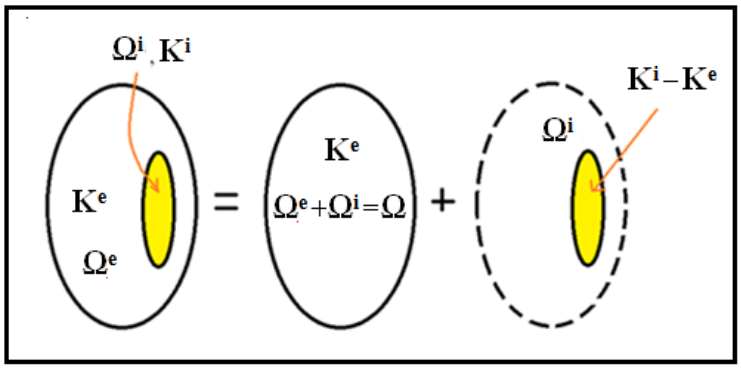

Figure 4: Complete and sectorial domains with homogeneous properties

In Fig. 4, the complete domain $\Omega(X)$ is composed by the sum of Ω^e and Ω^i; both K^e and K^i are physical properties, constant inside each sub-domain. In this formulation, unlike what is done in sub-regions, a complete or surrounding domain is elected; such is shown above, with homogeneous properties, e.g., K^e.

Consider that the kernel of the integrals is comprised by integrable functions. Supposing then $K^i=K^e+K^*$, the following equations can be written:

$$\begin{aligned}
&\int_{\Omega} K(X)\mathrm{u}(\mathrm{X})_{,\mathrm{ii}}\, u^*(\xi;\mathbf{X})d\Omega(\mathbf{X}) = \\
&K^e \int_{\Omega^e} \mathrm{u}^{\mathrm{e}}(\mathrm{X})_{,\mathrm{ii}}\, u^*(\xi;\mathbf{X})d\Omega^e(\mathbf{X}) + K^i \int_{\Omega^i} \mathrm{u}^{\mathrm{i}}(\mathrm{X})_{,\mathrm{ii}}\, u^*(\xi;\mathbf{X})d\Omega^i(\mathbf{X}) = \\
&K^e \int_{\Omega^e} \mathrm{u}^{\mathrm{e}}(\mathrm{X})_{,\mathrm{ii}}\, u^*(\xi;\mathbf{X})d\Omega^e(\mathbf{X}) + \int_{\Omega^i} (K^e + K^*)\mathrm{u}^{\mathrm{i}}(\mathrm{X})_{,\mathrm{ii}}\, u^*(\xi;\mathbf{X})d\Omega^i(\mathbf{X}) = \\
&K^e \int_{\Omega} \mathrm{u}^{\mathrm{e}}(\mathrm{X})_{,\mathrm{ii}}\, u^*(\xi;\mathbf{X})d\Omega^e(\mathbf{X}) + K^* \int_{\Omega^i} \mathrm{u}^{\mathrm{i}}(\mathrm{X})_{,\mathrm{ii}}\, u^*(\xi;\mathbf{X})d\Omega^i(\mathbf{X}) = 0
\end{aligned} \tag{10}$$

Now, the property K^e comprises the complete domain and thus no interface exist inside it; consequently, in this homogeneous model there is no additional numerical approximation beyond the usual ones carried on the external boundary. Eliminating K*, it results:

$$\mathrm{K}^{\mathrm{e}} \int_{\Omega} \mathrm{u}(\mathrm{X})_{,\mathrm{ii}}\, \mathrm{u}^*(\xi;\mathbf{X})\mathrm{d}\Omega(\mathbf{X}) = (\mathrm{K}^{\mathrm{e}} - \mathrm{K}^{\mathrm{i}}) \int_{\Omega^{\mathrm{i}}} \mathrm{u}^{\mathrm{i}}(\mathrm{X})_{,\mathrm{ii}}\, \mathrm{u}^*(\xi;\mathbf{X})\mathrm{d}\Omega^{\mathrm{i}}(\mathbf{X}) \tag{11}$$

Equation 11 could have been proposed and interpreted by energy principles. In the BEM, the integral equation is related to the equilibrium of energy in the system. As it stands, there is equilibrium of diffusive energy and work of fluxes on both sides of equality given by Eq. 11. In the proposed method it is necessary only the evaluation of the quantity the diffusive energy present in the involved sub-domain, such as is done in the accounting of the work due to a source or any external action in Poisson's problems.

For clarify ideas, the right hand side of Eq. 11 is rewritten in boundary integral form, considering the source points located externally to $\Omega_i(X)$ for sake of simplicity:

$$\begin{aligned}
&(\mathrm{K}^{\mathrm{e}} - \mathrm{K}^{\mathrm{i}}) \int_{\Omega^{\mathrm{i}}} \mathrm{u}^{\mathrm{i}}{}_{,\mathrm{ii}}(\mathbf{X})\mathrm{u}^*(\xi;\mathbf{X})\mathrm{d}\Omega^{\mathrm{i}}(\mathbf{X}) = (\mathrm{K}^{\mathrm{e}} - \mathrm{K}^{\mathrm{i}})[\int_{\Gamma^{\mathrm{i}}} \mathrm{q}^{\mathrm{i}}(\mathbf{X})\mathrm{u}^*(\xi;\mathbf{X})\mathrm{d}\Gamma^{\mathrm{i}}(\mathbf{X}) \\
&- \int_{\Gamma^{\mathrm{i}}} \mathrm{u}^{\mathrm{i}}(\mathbf{X})\mathrm{q}^*(\xi;\mathbf{X})\mathrm{d}\Gamma^{\mathrm{i}}(\mathbf{X})]
\end{aligned} \tag{12}$$

The first boundary integral on the right hand side of Eq. 12 represents the work of fluxes $q^i(X)$, while the other integral represents the diffusive energy that is expressed as a function of potentials $u^i(X)$. Together, these integrals are self-compensated, because the work of fluxes that reach the border is balanced by changes in the diffusive energy inside the Ω_i domain. The purpose of this method is to evaluate just one of these kinds of energy. This is much easier to make if is considered only the diffusive energy, since it is given as a function of the potentials at internal points, whilst dealing with normal fluxes is more cumbersome.

Thus, in this proposed model the energy stored in the non homogeneous sector is given just by the internal potentials $u_i(X)$. The complete integral equation will be in the form as follows:

$$c(\xi)u(\xi) + \int_{\Gamma} u(\mathbf{X})q^*(\xi;\mathbf{X})d\Gamma(\mathbf{X}) - \int_{\Gamma} q(\mathbf{X})u^*(\xi;\mathbf{X})d\Gamma(\mathbf{X}) = -\frac{(K^e - K^i)}{K^e}\int_{\Gamma^i} u^i(\mathbf{X})q^*(\xi;\mathbf{X})d\Gamma^i(\mathbf{X}) \tag{13}$$

Notice that the work of fluxes in internal boundaries is not null, but the energy contribution of non homogeneous sector in the energy balance in the whole system - which is not yet known – is done just advantageously by the diffusive energy. The two integrals and the point function on the left hand side of Eq. 13 are affected by the diffusive energy introduced by the sub-domain, so that the system responds as a whole, i.e., potential and fluxes calculated by the final system of equations take into account the effect of all the sub-domains and the surrounding domain as well.

Since the sectorial energy is represented exclusively through potential values at internal points rather than potential derivatives, the assembly of the complete system of equations is facilitated. It is important to observe that in this numerical procedure, the values at internal points should be calculated simultaneously with boundary nodal points. Notice that internal points unknowns appear explicitly in the final BEM system, that is, together with boundary nodal points, as shown in Eq. 14, by submatrix H_{ic}:

$$\begin{pmatrix} \mathbf{H}_{cc} & \mathbf{H}_{ci} \\ \mathbf{H}_{ic} & \mathbf{H}_{ii} \end{pmatrix} \begin{pmatrix} \mathbf{u}_c \\ \mathbf{u}_i \end{pmatrix} = \begin{pmatrix} \mathbf{G}_{cc} & \mathbf{0}_{ci} \\ \mathbf{G}_{ic} & \mathbf{0}_{ii} \end{pmatrix} \begin{pmatrix} \mathbf{q}_c \\ \mathbf{q}_i \end{pmatrix} \tag{14}$$

In the above equation, u_i are the potential at internal points that define the sectorial boundary $\Gamma_i(X)$ of the region $\Omega_i(X)$; u and q are values at nodal points on the boundary $\Gamma(X)$. Such as occur with the sectorial body loads, it is necessary to transmit information from the sectorial domain $\Omega_i(X)$ to the complete domain $\Omega(X)$; thus, the submatrix Hci represents coefficients generated by integration on internal boundaries $\Gamma_i(X)$ with source points based on boundary nodes belonging to surrounding boundary $\Gamma(X)$.

Although Eq. 11 has been written for the source points located externally to $\Omega_i(X)$, such source points are also positioned internally, performing a typical BEM scanning on the sub-domain boundaries, represented in Eq. 14 by submatrix H_{ii}. Differently from what occurs with the sub-regions technique, since all internal and boundary source points interact each with other, the matrix H is completely filled.

Finally, for source points located exclusively outside the sectorial domain, the values of $c(\xi)$ for the integral equation related to H_{ci} are null. However, in the cases where some part of the involved boundary $\Gamma_i(X)$ has an intersection with $\Gamma(X)$, the coefficients $c(\xi)$ can be calculated by standard BEM procedures.

For better understanding, the components of complete matrix H generated by a simple mesh that represents a square domain with four straight constant boundary

elements and four internal points are shown in Fig. 5. In this matrix easily can be observed the diagonal components of submatrices H_{cc}, H_{ci} and H_{ii} (see Eq. 14), which reflect clearly the use of constant boundary elements.

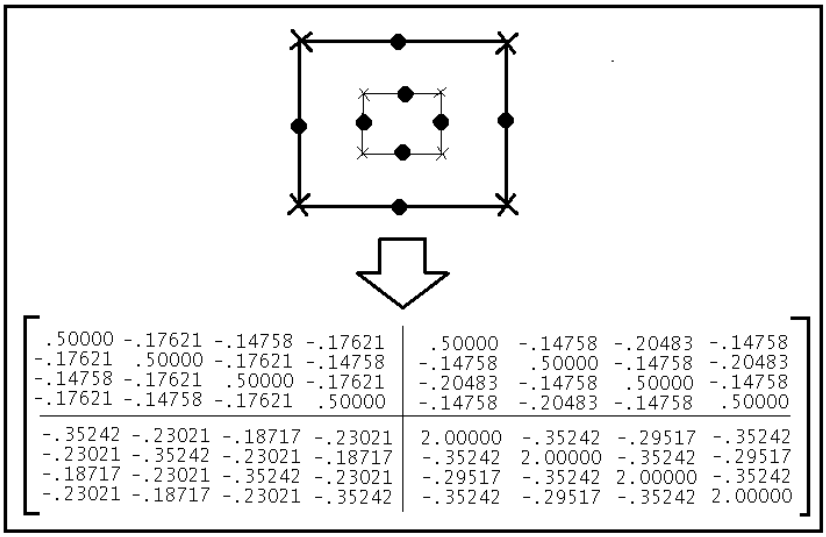

Figure 5: H matrix concerning a discretization of a square domain using four boundary elements and four internal points

In the proposed model, all points, boundary and internal points, are taken as source points. Differently from what occurs with the sub-regions technique, since all internal and boundary source points interact each with other, the matrix H is completely filled. This is one reason to justify the better accuracy of proposed technique. The size of final matrices in the proposed technique is slightly smaller than size of sub-regions matrices, since the fluxes in internal points are not included.

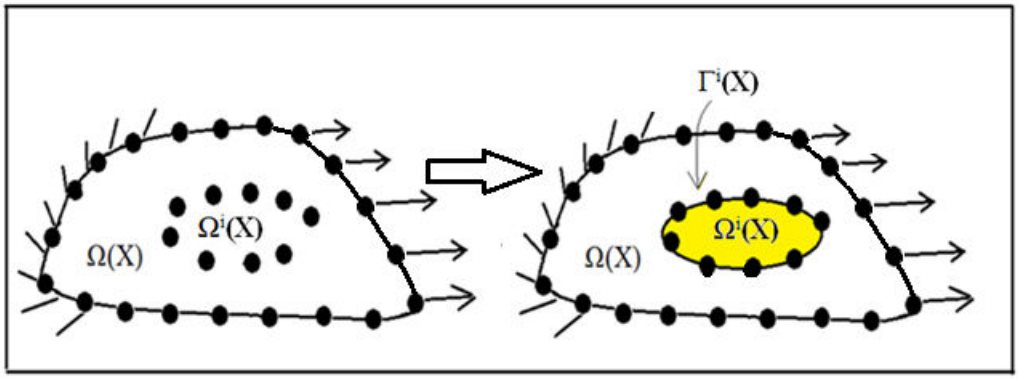

Figure 6 – Internal points are arranged to define the shape of the boundary of the heterogeneous region Ωi(X).

The second reason for better accuracy is related to absence of internal discretization in the complete or surrounding domain. Indeed, an internal interpolation is created by generation of sub-domains through linkage between adjacent internal points (see Fig. 6);

however, one part of problem, that is, the surrounding domain, is solved such as a homogeneous Laplace's problem.

4 NUMERICAL SIMULATIONS

Simple problems with regular geometry were chosen to comparison between the Sub-regions Technique and proposed methodology. It is used straight constant boundary elements for simulations. As measure of error, it was used the following formula, in which the maximum value of reference was used as denominator and the modulus of the difference between the reference and numerical values comprises the numerator:

$$\text{Error} = \sum_{n=1}^{N} \frac{|u_{\text{reference}} - u_{\text{numerical}}|}{N * \text{valor max}(u_{\text{referência}})} \qquad (15)$$

Values of reference were composed by the analytical solution, if available, or then by results given by the Finite Element Method, using a finer mesh with linear interpolation. Boundary element meshes with different level of refinement were solved to generate a suitable average error curve.

4.1 First Example

The first simulation shows a bar with two sectors with different properties. The geometry of the problem, as well as the boundary conditions and property values of each sector are shown in Figure 7.

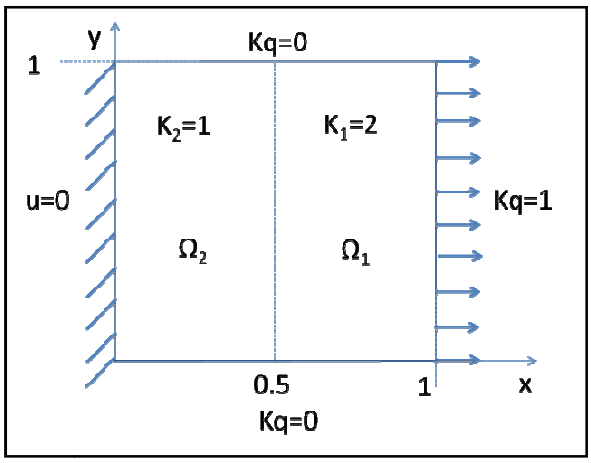

Figure 7: Unitary bar with two different sectors Ω_1 e Ω_2

The number of boundary nodes for each mesh is shown on the abscissa of the graph of figure 8, while the ordinate indicates the relative error committed in the potential calculated on the vertical lines.

From these results it is possible to show that, for both techniques, the error value decreases with increasing the number of boundary nodes; however, the most relevant point is that the error curve achieved using the new formulation. Even with a coarse discretization, the values of error relative are very low. This trend continued with the increasing number of boundary elements.

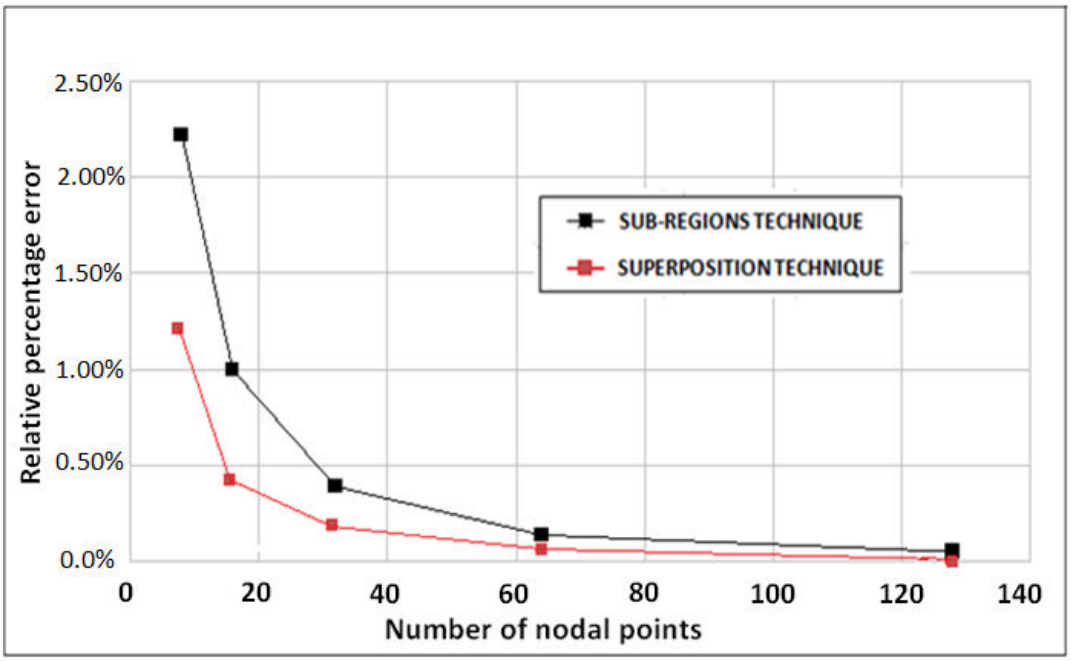

Figure 8: Relative average error curve as a function of number of boundary nodes

4.2 Second Example

This two-dimensional problem can be understood as a square sheet with unitary sides, in which the potential is prescribed on just a unique side and normal derivatives of potential are prescribed on other sides. An internal sector with stiffness K* is located centered in the sheet, as shown in Fig. 9.

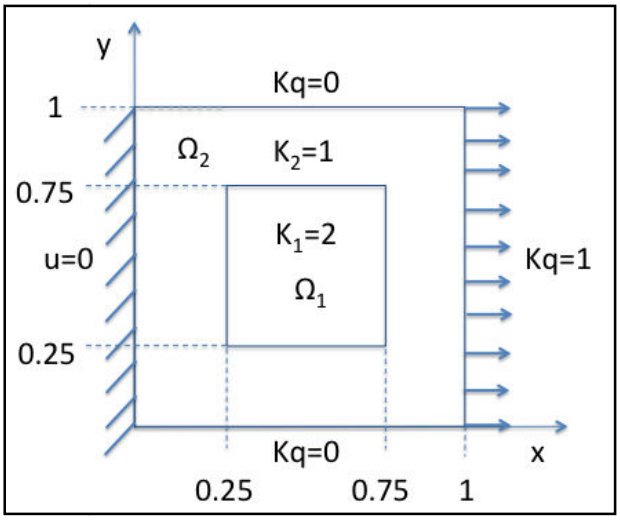

Figure 9: Surrounding domain Ω_2 with sector Ω_1.

The reference solution now is given by the Finite Element Method (Reddy, 2005). A mesh with 3200 linear finite elements and 1681 nodes was used as benchmark to check boundary element accuracy.

The results were taken along the vertical line at y = 1. The relative error between the results obtained through the FEM and simulated values for the sub-region techniques and novel formulation are shown in Figure 10.

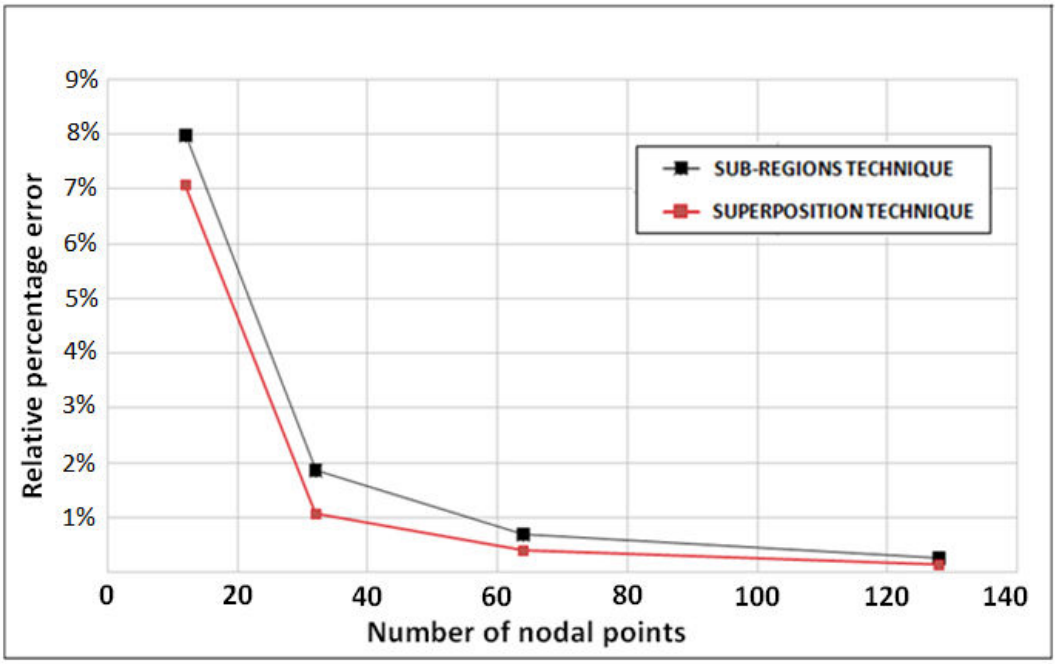

Figure 10: Unitary square sheet with internal sector with different physical property.

The result shown is similar to that found in the previous example. For both boundary techniques, the error value decreases with increasing the number of nodes, as expected. However, again, the most important point is the performance of the error curve achieved by the new formulation. Even with a low discretization error figures are very low. This trend is continued with the increasing number of elements.

4.3 Third Example

In this example, the surrounding domain possesses two internal domains with different physical properties. Figure 11 shows the geometric features and boundary conditions for this case.

The reference solution now was given by solution given by the Finite Volume Method (LeVeque, 2007), using a structured mesh with 1664 rectangular cells. For both boundary element formulations, were used meshes with 38 and 76 boundary nodes. The error values were calculated using the numerical results for potential obtained along nodal points located on the vertical line at y=0. Table 1 shows the average error curve.

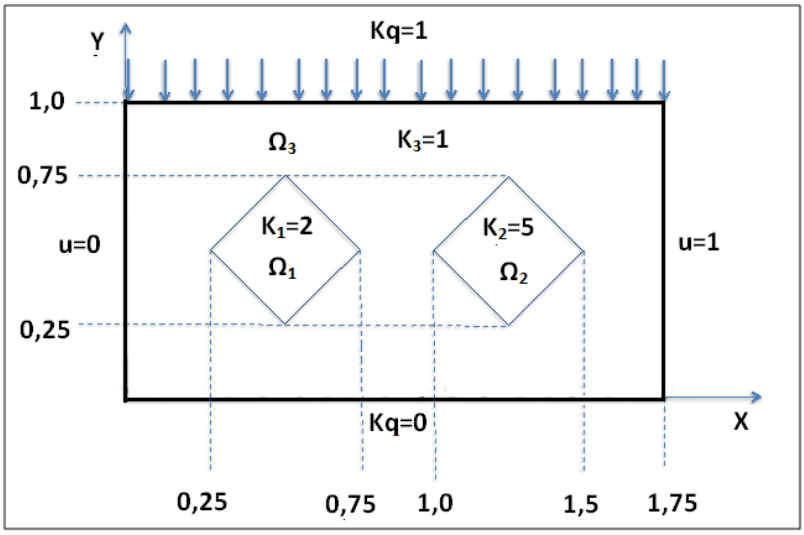

Figure 11: Surrounding domain with two sub domains with different physical properties

Again it can be realized that the results of both BEM techniques has good performance, quite close to the reference value. The proposed technique has inferior performance for finer mesh; however, considering the level of errors, it is possible that the Finite Volume mesh used here does not present enough accuracy to serve as undoubted reference.

Table 1: Relative errors for Sub-Region and Superposition Technique.

Relative error (%)		
Number of nodal points	SUB-REGION	SUPERPOSITION TECHNIQUE
38	0,180%	0,162%
76	0,062%	0,070%

5 CONCLUSIONS

The numerical results achieved shown a very favorable performance of the new technique and ratify that it can used advantageously in problems in which the physical properties of the domain vary sectorally. The accuracy for the new technique was meaningful superior that the classical sub-region technique.

Besides good accuracy, the new method shows a significant advantage in terms of computational implementation and data entry due to its simplicity. To implement the proposed model, it is necessary only the generation of a new kind of matrix H, that contains the potential energy related to the internal sectors, and to add it to classic BEM system.

The present technique produces less severe approximation in numerical model than the classic technique of sub-regions, since due to the superposition of domains, the surrounding area remains free of internal interfaces. Only the sub-domains introduce geometric interpolation due to connection between adjacent internal points to form the boundaries.

The good accuracy of the proposed technique can also be attributed to the fact that all the nodes interact with each other; however, if desired, only a restricted number of selected points can interact with the nodes belonging to the sub domains, despite to the numerical precision decrease in this case.

The proposed procedure also does not create any impediment to the implementation of auxiliary procedures such as the Dual Reciprocity Technique, the DIBEM (Loeffler et al., 2015) or any other suitable methodology to address more advanced problems. There is a significant potential in the new technique with respect to future applications of great interest and complexity, particularly in the elastic-plastic analysis and structural dynamics.

This scope of this work was the modeling of the Laplace equation in two dimensions, but relatively simple future works can be performed dealing with the proposed method approaching three dimensions or correlate scalar field equations, such as Poisson's Equation and the Helmholtz Equation. Application to the stationary form of Navier's Equation, this last belonging to the elasticity problems is also very accessible.

REFERENCES

Brebbia, C. A., Dominguez, J., 1992. *Boundary Elements – An Introductory Course*, WIT Press.

Brebbia, C. A., Telles, J. C. F., & Wrobel, L. C., 1984. *Boundary Element Techniques.* Springer-Verlag, Berlin.

Brebbia, C. A., Walker, S., 1980. *Boundary Element Techniques in Engineering*, Newnes-Butterworths, London.

Kythe O. J., 1995. *An Introduction to Boundary Element Methods*, CRC Press, Boca Ratton.

LeVeque R., 2007. *Finite Difference Methods for Ordinary and Partial Differential Equations: Steady-State and Time-Dependent Problems*, SIAM, Philadelphia.

Loeffler, C. F., Cruz, A. L., Bulcão, A. 2015. Direct Use of Radial Basis Interpolation Functions for Modelling Source Terms with the Boundary Element Method. *Eng. Analysis with Boundary Elements*. v. 50, pp.97-108.

Loeffler C. F., Mansur W. J., 1987. Uma Nova Abordagem do Método dos Elementos de Contorno para Solução de Problemas com Cargas de Domínio. *Anais do VIII Congresso Latino- Americano e Ibérico sobre Métodos Computacionais para Engenharia*, Rio de Janeiro, v. B, pp. 347-362.

Paiva J. B., Venturini W. S., 1993. Alternative boundary element approach to compute efforts along zoned domain interfaces. *Eng. Analysis with Boundary Elements,* v. 12, pp. 143-148.

Partridge, P. W., Brebbia, C. A., & Wrobel, L. C., 1992. *The Dual Reciprocity Boundary Element Method.*Comput. Mechanics Publications and Elsevier, London.

Ramachandran, P. A., 1994. *Boundary Element Methods in Transport Phenomena*, 1st Ed. Computational Mechanics Publication and Elsevier Applied Science, London, UK.

Reddy J., 2005. *An Introduction to the Finite Element Method*, McGraw-Hill, New York.

Wrobel, L.C., Aliabadi, M.H., 2002. *The Boundary Element Method*, Wiley, Chichester.

Xiaoping L., Wei-Liang W., 2005.A new sub-region Boundary Element Technique based on the Domain Decomposition Method. *Eng. Analysis with Boundary Elements*, v. 29, pp. 944–952.